

Article

Dehydration Sensitivity at the Early Seedling Establishment Stages of the European Beech (*Fagus sylvatica* L.)

Ewa M. Kalemba ^{1,*}, Agnieszka Bagniewska-Zadworna ², Jan Suszka ¹ and Stanisława Pukacka ¹

¹ Institute of Dendrology, Polish Academy of Sciences, Parkowa 5, 62-035 Kórnik, Poland; jsuszka@man.poznan.pl (J.S.); spukacka@man.poznan.pl (S.P.)

² Department of General Botany, Institute of Experimental Biology, Faculty of Biology, Adam Mickiewicz University, Umultowska 89, 61-712 Poznań, Poland; agabag@amu.edu.pl

* Correspondence: kalemba@man.poznan.pl; Tel.: +48-61-8170033

Received: 4 September 2019; Accepted: 9 October 2019; Published: 11 October 2019



Abstract: Shortage of water is a limiting factor for the growth and development of plants, particularly at early developmental stages. We focused on the European beech (*Fagus sylvatica* L.), which produces seeds and further seedlings in large intervals of up to ten years. To explore the beech seedling establishment process, six stages referring to embryo expansion were studied to determine sensitivity to dehydration. The characterization of the response of elongating embryonic axes and cotyledons included a viability test before and after dehydration and measurement of the amounts of electrolyte leakage, concentration, and arrangement of storage materials, changes in chaperone proteins related to water deficit, and accumulation of hydrogen peroxide and superoxide anion radicals. Elongating embryonic axes and cotyledons differed in water content, dehydration rates, membrane permeability before and after dehydration, protein, and lipid decomposition pattern, and amount of 44-kDa dehydrin and 22-kDa small heat shock protein (sHSP). Protruding embryonic axes were more sensitive to dehydration than cotyledons, although dehydration caused transient reinduction of three dehydrin-like proteins and sHSP synthesis, which accompany desiccation tolerance. Extended deterioration, including overproduction of hydrogen peroxide and depletion of superoxide anion radicals, was reported in dehydrated embryonic axes longer than 10 mm characterized by highly elevated cellular leakage. The apical part elongating embryonic axes consisting of the radicles was the most sensitive part of the seed to dehydration, and the root apical meristem area was the first to become inviable. The effects of severe dehydration involving ROS imbalance and reduced viability in beech seedlings with embryonic axes longer than 10 mm might help to explain the difficulties in beech seedling establishment observed in drought-affected environments. The conversion of environmental drought into climate-originated oxidative stress affecting beech seedling performance is discussed in this report.

Keywords: dehydrin-like proteins; small heat shock proteins; storage materials; lipids; reactive oxygen species; viability

1. Introduction

Desiccation tolerance enables survival in the face of severe dehydration without consequent water stress [1]. Orthodox seeds acquire desiccation tolerance during maturation, remain tolerant in a dry state and after release from dormancy until the beginning of radicle protrusion in germinating seeds [2]. Desiccation tolerance is not further sustained at the seedling stage, making the seedling establishment

stage the most sensitive to water limitations. During development, beech (*Fagus sylvatica* L.) seeds acquire dormancy and desiccation tolerance [3]. However, beech seeds belong to the intermediate category due to their poor longevity during storage under typical conditions compared to orthodox seeds [4]. Dormancy facilitates the survival of seeds in a dry state during unfavorable conditions and subsequently enables germination and efficient beech reproduction. Unfortunately, a good cropping year occurs only once every 10 years, and extreme interannual variation in seed production is mainly caused by deficiencies in pollen synthesis [5]. The seedling formation is additionally hampered by the fact that the growth of beech trees is sensitive to global environmental changes [6]. The European Environment Agency states that Europe has warmed more than the global average. In this context, the natural environmental conditions are inconsistent with the optimal storage conditions (7.8%–11.5% of water content at -10 to -20 °C) established for beech seeds [4,7], limiting successful production of high quality seedlings and natural regeneration of beech trees, even if it is combined with site preparation [8]. Moreover, forestation practice is based on long-term stored beech seeds from seedbanks, often representing lowered quality. Thus, to maximize the success of beech seedling performance, it was necessary to determine the most limiting factor. The environmental drought became a candidate in our study because soil water content lower than 12% significantly reduces seed germination and seedling emergence [9].

The tri-phasic seed germination model comprises seed imbibition manifested by water uptake (first phase), germination *sensu stricto* (second phase) and postgermination growth (third phase), which refers to a further increase in water uptake that results in embryo expansion [10]. The emergence of radicles begins at the second/third phase edge, and rapid growth is reported during the third phase, which we investigated. Arabidopsis mutant studies revealed that proper storage reserve mobilization in germinating oilseeds is essential for germination initialization and normal seedling establishment [11]. In addition, the accumulation of storage materials has important protective benefits during dehydration and desiccation [12]. Actually, the germination capacity of beech seeds is related to lipid composition [13] and protein metabolism [14]. The above data encouraged us to investigate the level of lipids in beech during dormancy breaking and the three germination phases when growth processes consume this energy source, desiccation tolerance is gradually lost and dehydration-sensitive seedlings are produced [10,15] to examine whether the germination program is executed properly.

Desiccation tolerance acquisition and loss are precisely controlled genetically by mechanisms related to the activation of protective mechanisms [16], including macromolecule stabilization by chaperones [17]. Some members of two large protein families, late embryogenesis abundant (LEA) proteins and small heat shock proteins (sHSP), expressed in seeds, play an important role in desiccation tolerance acquisition [15,18]. Particularly in group II of the LEA group, some specific dehydrins are involved in the desiccation tolerance trait in seeds [19], while others are expressed in vegetative tissues and in desiccation-sensitive tissues in response to osmotic stress. Dehydrins protect cellular macromolecules and membranes and might act as antioxidants and membrane and protein stabilizers ([19] and references therein). Using antibodies specific to the K segment [20], at least four dehydrin-like proteins with approximate molecular weights of 26, 35–37, 40, and 44-kDa were detected in beech seeds during development [3,21] and during storage [22], with higher amounts in embryonic axes. The 44 and 26-kDa proteins were heat-stable dehydrins and were experimentally confirmed to be a homodimer and monomeric form, respectively, of dehydrin/response ABA protein belonging to the Y_nSK_2 subgroup of dehydrins [23], which was reported to be particularly induced by drought [24]. sHSPs are associated with the general mechanism of cellular response to abiotic stress [18]. These proteins can attach to denatured proteins, prevent aggregation, stabilize conformations and assist in protein folding, oligomer formation, and intracellular transport, all of which are important during desiccation and germination [15,25,26]. Dry beech seeds contained 22-kDa sHSP, and considerably higher levels of the protein were detected in embryonic axes [22]. The important information was lacking: how long can the two classes of chaperones linked to water deficits in seeds support tolerance to dehydration in beech seedlings? Based on the proteomic data from the seeds of eight species, including beech,

molecular processes occurring during germination in response to environmental factors were identified, i.e., osmotic homeostasis that included dehydrins and the protein processing category that included sHSPs [27], thereby emphasizing the necessity and validity of our research.

Long-term stored beech seeds are unable to germinate due to oxidation effects on protein synthesis, folding and degradation [28]. Reactive oxygen species (ROS) exhibit a dual role in seed physiology [29]. Depending on the concentration, ROS are considered second messengers or agents introducing oxidative stress. Bailly et al. [30] established the concept of the "oxidative window for germination" linked to a specific range of ROS levels, which leads to the initiation and further progress of seed germination. ROS, including hydrogen peroxide (H_2O_2), superoxide anion radical ($O_2^{\bullet-}$) and hydroxyl radical ($\cdot OH$), are involved in the germination process in seeds, particularly in root development [31–33]. Furthermore, H_2O_2 , $O_2^{\bullet-}$, and $\cdot OH$ are essential for the normal growth and development of seedlings [34]. Dehydration of desiccation-sensitive seeds causes higher ROS production in comparison to desiccation-tolerant seeds [35]. Moreover, ROS accumulation and oxidative stress injury are the main causes of beech seed aging [36]. In this context, it was necessary to compare the pattern of ROS production at early seedling developmental stages under normal conditions and after severe dehydration to determine whether water stress is followed by oxidative stress and contributes to viability. Moreover, ROS induced lipid peroxidation impacts membrane integrity and results in cellular leakage [37]. Thus, electrolyte leakage, as one of the plant stress biomarkers used to quantify dehydration-induced damage [38] and decline in viability [39,40], was applied in this study.

We focused on the characterization of the sensitivity of developing beech seedlings to dehydration to improve the understanding of natural regeneration with implications for forestry. Studies concerning *Arabidopsis* seed germination revealed that the root tip of radicle functions in germination initiation [41], but cell expansion and completion of germination are located in the lower hypocotyl and hypocotyl-radicle transition zone [42]. To address the question of whether any desiccation tolerance-related symptoms might be detected at early stages of beech seedling establishment, dehydration tolerance loss in cotyledons and radicles divided into zones was investigated. By investigating dehydration tolerance, we determined that separated radicles and cotyledons differ in (1) sensitivity to dehydration, (2) hydration and dehydration rates, (3) amounts of electrolyte leakage before and after dehydration, (4) viability, (5) expression of chaperone proteins related to desiccation tolerance upon dehydration, (6) depletion of storage materials, (7) arrangement of lipid storage materials, and (8) perturbations in ROS levels caused by dehydration. The above results emphasize that differences in dehydration tolerance of two seed tissues contribute to the success of seedling performance. The effects of severe dehydration involving ROS imbalance and reduced viability in beech seedlings with radicles longer than 10 mm limit beech seedling establishment in drought-affected environments.

2. Materials and Methods

2.1. Material Preparation

Seeds of the European beech (*Fagus sylvatica* L.) stored at $-10\text{ }^\circ\text{C}$ and 10% water content (WC) and characterized by $95\% \pm 1\%$ germination capacity were used in all experiments. Seeds originated from a single tree growing in the Kórnik Arboretum (West Poland). Seeds were moistened up to 30% WC, placed in closed plastic boxes (3×1000 seeds each) and subjected to cold stratification ($3\text{ }^\circ\text{C}$) and a 12 h light/12 h dark cycle to lead the germination process. Seeds began to germinate at the 10th week, at which point the seed samples were collected and classified depending on the elongating embryonic axis length (stage 0—3 mm, stage I—7 mm, stage II—10 mm, stage III—15 mm, stage IV—20 mm, stage V—25 mm) specified in Figure S1. At each collection, the WC was examined separately in radicles and cotyledons. To prepare seed samples for protein extraction, electrophoresis and Western blot analyses, the seed coats were removed, and the elongating embryonic axes were separated from cotyledons. Embryonic axes that elongated to 10 mm and longer were further divided into two parts:

apical part (A), containing the root tip of radicle, and distal part (D), containing hypocotyls. Individual elongating embryonic axes separated from cotyledons, elongating embryonic axes cut into A and D and cotyledons were used as seed samples. One portion of the seed samples representing physiological conditions (three replicates of 10 cotyledons and 20 elongating embryonic axes for each analysis) was weighed and frozen, and the remaining seeds were subjected to desiccation and sampled identically to analyze desiccation conditions.

2.2. Seed Viability after Dehydration

Dehydration of seed samples to 11% WC was performed at 20 °C over saturated solutions, enabling severe drying to mimic sudden environmental drought. Saturated solutions of potassium carbonate and sodium chloride resulting in relative humidities of 45% and 75% were used for embryonic axes or radicles and cotyledons, respectively, and were prepared according to water sorption isotherms established separately for embryonic axes and cotyledons of beech seeds [7]. The initial WC of seed samples intended for dehydration was determined using a moisture meter (Sartorius MA100, Sartorius Lab Instruments, Göttingen, Germany). Seed samples were weighed (FW, fresh weight) before the dehydration process began. Based on the WC and FW values, dry weight (DW) and the expected weight of seed samples corresponding to 11% WC were calculated. The water loss was monitored by weighting the samples every 1–2 h during the day with an interval of 8 h at night. The triphenyl tetrazolium chloride (TTC) dye test [43] was used to assess seed viability before and after dehydration. Dried seeds were slowly hydrated on fully moistened paper towels placed in Petri dishes. Seeds were transferred to paper towels moistened with 1% TTC in potassium phosphate buffer (pH 7.0), kept in darkness for 24 h and photographed. Tissues colored dark pink after dyeing were recognized as viable, while others were recognized as nonviable. TTC-stained cotyledons and elongating embryonic axes were incubated in 96% ethanol to extract the dark pink formazan for 24 h at darkness and gentle shaking. One cotyledon or five elongating embryonic axes per 1 mL were used for quantification. The absorbance of the solution was measured at 530 nm according to the method described by Chen et al. [44], in which viability was expressed as the ratio of absorbance obtained from dehydrated to nondehydrated control seed tissues.

2.3. Electrolyte Leakage

Three samples of ten elongating embryonic axes and five cotyledons were placed in 10 mL of deionized water. The electrical conductivity of the solutions was measured after 24 h of incubation at room temperature using a SevenEasy S20 (Mettler Toledo, Mettler-Toledo GmbH, Giessen, Germany) device equipped with an InLab®730 (Mettler-Toledo GmbH, Giessen, Germany) conductivity probe. The results are expressed as $\text{mS g}^{-1} \text{DW}$.

2.4. Protein Extraction

Seed samples of 20 elongating embryonic axes or radicles and 10 cotyledons were ground to a powder in liquid nitrogen. The dried powder was homogenized at 4 °C in a 1:2 (w:v) extraction buffer containing 20 mM Tris-Cl (pH 7.5), 5% glycerol, 1% protease inhibitor cocktail (Sigma-Aldrich, St. Louis, USA) and 1.5% polyvinylpyrrolidone (Sigma-Aldrich, St. Louis, USA). The samples were further centrifuged at $20,000 \times g$ for 20 min at 4 °C. To obtain heat-stable proteins, the supernatant was boiled for 10 min, cooled on ice for 15 min and centrifuged as described above [20]. The protein concentration was measured using the 2-D Quant Kit based on protein-catalyzed reduction of cupric (Cu^{2+}) ion to cuprous (Cu^{+}) ion.

2.5. Electrophoresis

Proteins were separated using 4%–15% polyacrylamide gels. Tris-glycine-sodium dodecyl sulfate (SDS) buffers were used to perform SDS-PAGE. Spectra™ Multicolor Broad Range Protein Ladder was used to estimate the protein molecular mass.

2.6. Western Blot Analysis

Antibodies against the dehydrin consensus K segment [20] and Arabidopsis Hsp 17.4 [25] were used at a 1:1000 dilution. The secondary antibody was conjugated with alkaline phosphatase (Sigma-Aldrich, St. Louis, USA) and used at a 1:10,000 dilution. The Western analysis was conducted as described in Kalemba and Litkowiec [23].

2.7. Lipid Extraction

Samples of 20 elongating embryonic axes or radicles and 10 cotyledons each were subjected to lipid extraction according to the procedure described in Ratajczak and Pukacka [13]. An aliquot of the lipid extract was transferred to preweighed aluminum pans, weighed, dried under the stream of gaseous nitrogen to evaporate the chloroform and weighed again to obtain the dried extract weight. The total lipid calculation was based on the equation considering the fresh weight of the seed sample assayed and presented as a percentage.

2.8. Ultrastructural Analyses

Samples were fixed in 2% glutaraldehyde and 2% formaldehyde (pH 6.8) overnight at 4 °C and postfixed with 1% osmium tetroxide for 2 h at room temperature for cytological studies. The fixed material was counterstained and embedded in low-viscosity resin using the method described by Bagniewska-Zadworna et al. [45]. Ultrathin sections (0.1 µm) were cut on an ultramicrotome EM UC6 (Leica-Reichert, Bensheim, Germany). The sections were stained with uranyl acetate and lead citrate and examined with a JEM 1200 EX II transmission electron microscope (Jeol, Tokyo, Japan) operating at an accelerating voltage of 80 kV.

2.9. Lipid Storage Material Visualization

For the detection of lipids in fresh sections of cotyledons and embryo axes, a histochemical reaction with 1% Sudan III in 70% ethanol was performed, as described by Krishnamurthy [46].

2.10. Histochemical Detection of ROS

Hydrogen peroxide (H₂O₂) was visualized in elongating embryonic axes by staining with 1 mg mL⁻¹ 3,3'-diaminobenzidine (DAB) solution in sodium phosphate buffer according to the method of Daudi and O'Brien [47] with several modifications. A gentle vacuum was applied for 30 min, and the time for DAB staining was extended to 24 h. The chlorophyll removal step was omitted. H₂O₂ was visualized as a reddish-brown stain formed by the reaction of DAB with endogenous H₂O₂. Superoxide anion radical (O₂^{•-}) was visualized using 0.2% nitroterazolium blue chloride (NBT) in sodium phosphate buffer (pH 7.5) using the protocol of Kumar et al. [48]. The accumulation of O₂^{•-} was visualized as dark blue to black stain formed by NBT reacting with endogenous O₂^{•-}. Photographs were made on a plain white background using a Nikon D3100 digital camera attached to a binocular.

2.11. Statistical Analysis

Data are presented as the means ± standard deviation of three biological replicates. The relationship between particular parameters was examined using Pearson's correlation coefficient analysis. The significance among the means of components was verified using analysis of variance (ANOVA) followed by Tukey's test at $p \leq 0.05$, and significantly different values were marked with different letters in the graphs.

3. Results

3.1. Water Status and Storage Materials under Normal Conditions

Germinated beech seeds were studied in six seedling establishment stages (0-V) referring to the third phase of germination manifested by embryonic axis protrusion. The water content was kept constant (30% WC) during cold stratification and was precisely monitored during the tested stages of seedling establishment (Figure 1A). A slight increase (36%–41%) was reported in cotyledons, whereas in the elongating embryonic axes, the increase was significantly larger (41%–74%) and linked to the radicle prolongation dynamics ($r = 0.70405$, $p = 0.02294$).

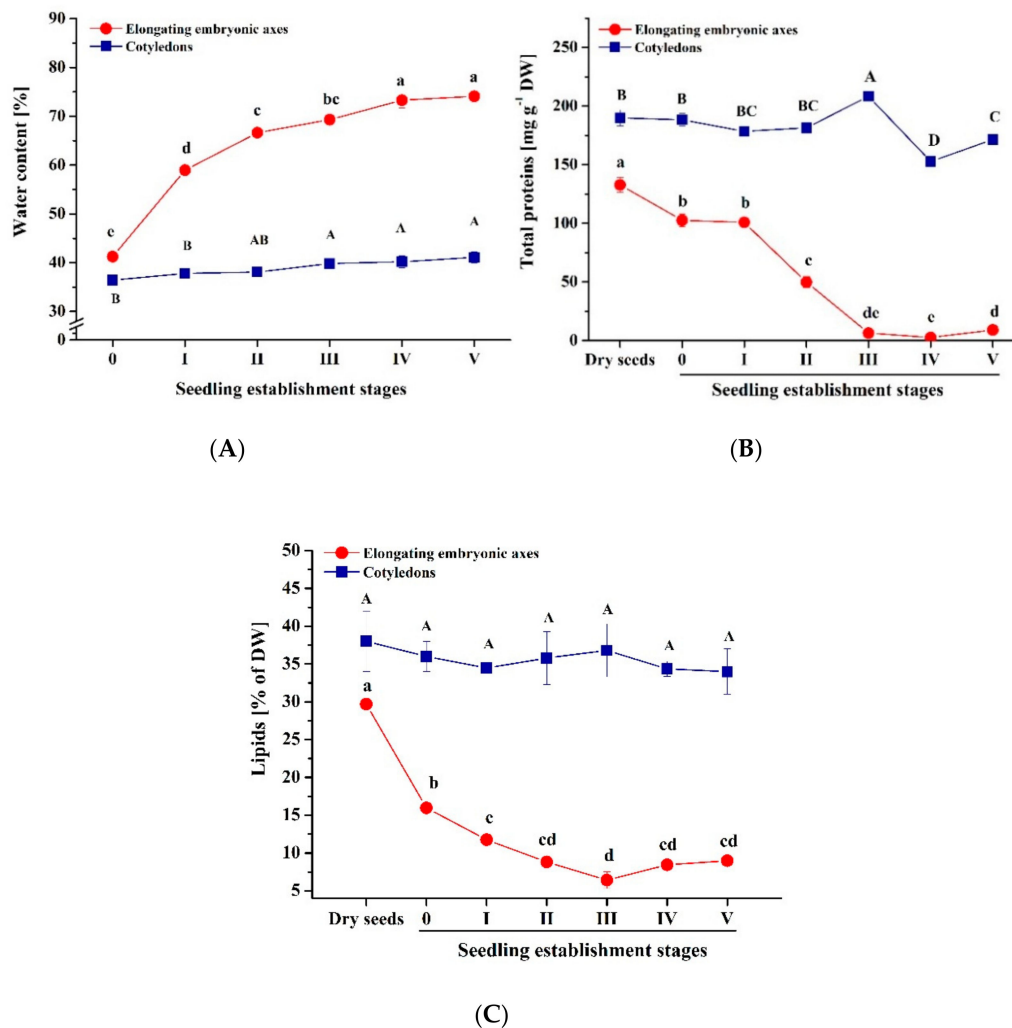


Figure 1. Changes in water status (A) and storage materials including proteins (B) and lipids (C) in elongating embryonic axes and cotyledons at selected seed germination and seedling establishment stages in *Fagus sylvatica* under normal conditions. Data shown as the means \pm standard deviation obtained from three independent experiments with similar results. Statistically significant differences are indicated with different letters (one-way ANOVA followed by Tukey's test at $p \leq 0.05$).

The level of storage materials was measured. The total protein level halved when embryonic axes protruded to 10 mm and continued to decrease at further seedling establishment stages as the embryonic axes prolonged ($r = -0.74443$, $p = 0.1689$). Changes in the protein levels of cotyledons were less pronounced (Figure 1B). Lipid depletion was monitored quantitatively (Figure 1C). Initially, lipids in cotyledons and embryonic axes in dry seeds constituted $38.1\% \pm 4.3\%$ and $29.6\% \pm 1.1\%$, respectively, of the dry weight. In cotyledons, the high level of lipids did not change significantly

during cold stratification, seed germination, and early seedling establishment stages, whereas in the embryonic axes, the lipids halved during cold stratification and continued to decrease at further stages.

3.2. Localization of Storage Materials

Transmission electron microscopy confirmed that epidermal cells were filled with oil bodies (Figure 2A,C). The increased number of oil bodies in cotyledons presumably contributed to a substantial reduction of cytoplasmic fluidity in this part of seed tissue (Figure 2A). In the embryonic axes, oil bodies formed one layer specifically in close proximity to the cell membrane in cells located in deeper layers (Figure 2D). In contrast, cotyledon cells also presented a higher number of oil bodies (Figure 2B). The contribution of the lipid storage material was additionally visualized using Sudan III staining and observed under a light microscope (Figure S2). Areas dyed orange and red pointed to the clearly different distribution of lipids in the cotyledons and embryonic axes. A higher concentration of lipids in external cell layers was evident in the cotyledons. Starch grains and protein vacuoles were less numerous than oil bodies.

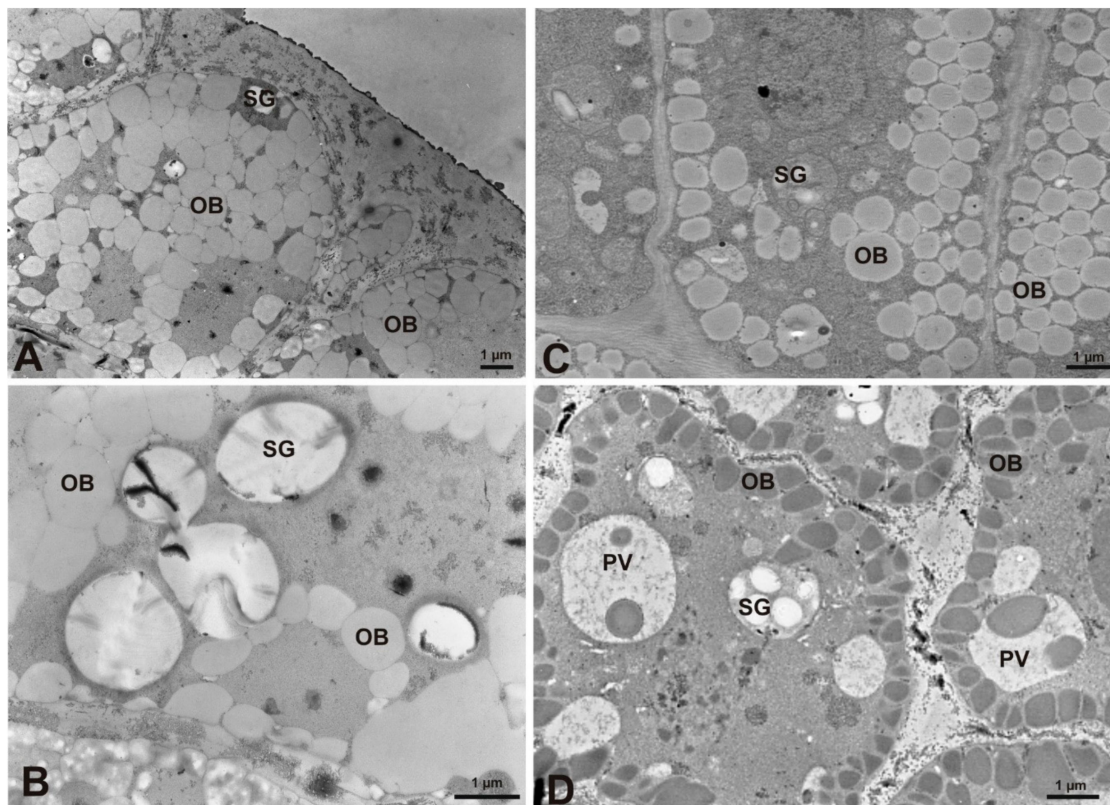


Figure 2. Ultrastructure of the cotyledons (A,B) and embryonic axes (C,D) of dry *Fagus sylvatica* seeds was performed to illustrate the arrangement of storage materials, especially oil bodies. Cells of the epidermal layer (A,C) and deeper layers (B,D) were visualized using transmission electron microscopy. Abbreviations: OB–oil body, SG–starch grain, PV–protein vacuole.

3.3. Response to Dehydration

Elongating embryonic axes and cotyledons differed in dehydration rates, reaching $56.7 \text{ mg H}_2\text{O g}^{-1}\text{DW h}^{-1}$ and $9.5 \text{ mg H}_2\text{O g}^{-1}\text{DW h}^{-1}$ on average, respectively, at seedling establishment stage 0 (Figure 3A). Beginning in stage II, the dehydration rates increased in elongating embryonic axes up to $270.5 \text{ mg H}_2\text{O g}^{-1}\text{DW h}^{-1}$ by seedling establishment stage V. At the 0–II stages of seedling establishment, the water was progressively lost in elongating embryonic axes, and a linear link with time was reported (Figure S3A). In contrast, a curve expressing water loss in time at seedling establishment stages IV–V showed a parabolic decrease. The differences in dehydration rates reported for cotyledons were less

pronounced (Figure S3B). In elongating embryonic axes, the amounts of electrolyte leakage were the lowest at the 0-I seedling establishment stages and did not differ between nondehydrated and dehydrated samples (Figure 3B). The gradual increase in electrolyte leakage from nondehydrated radicles began at seedling establishment stage II and was the most intense at stage V, being four times higher than at the beginning of embryonic axes protrusion.

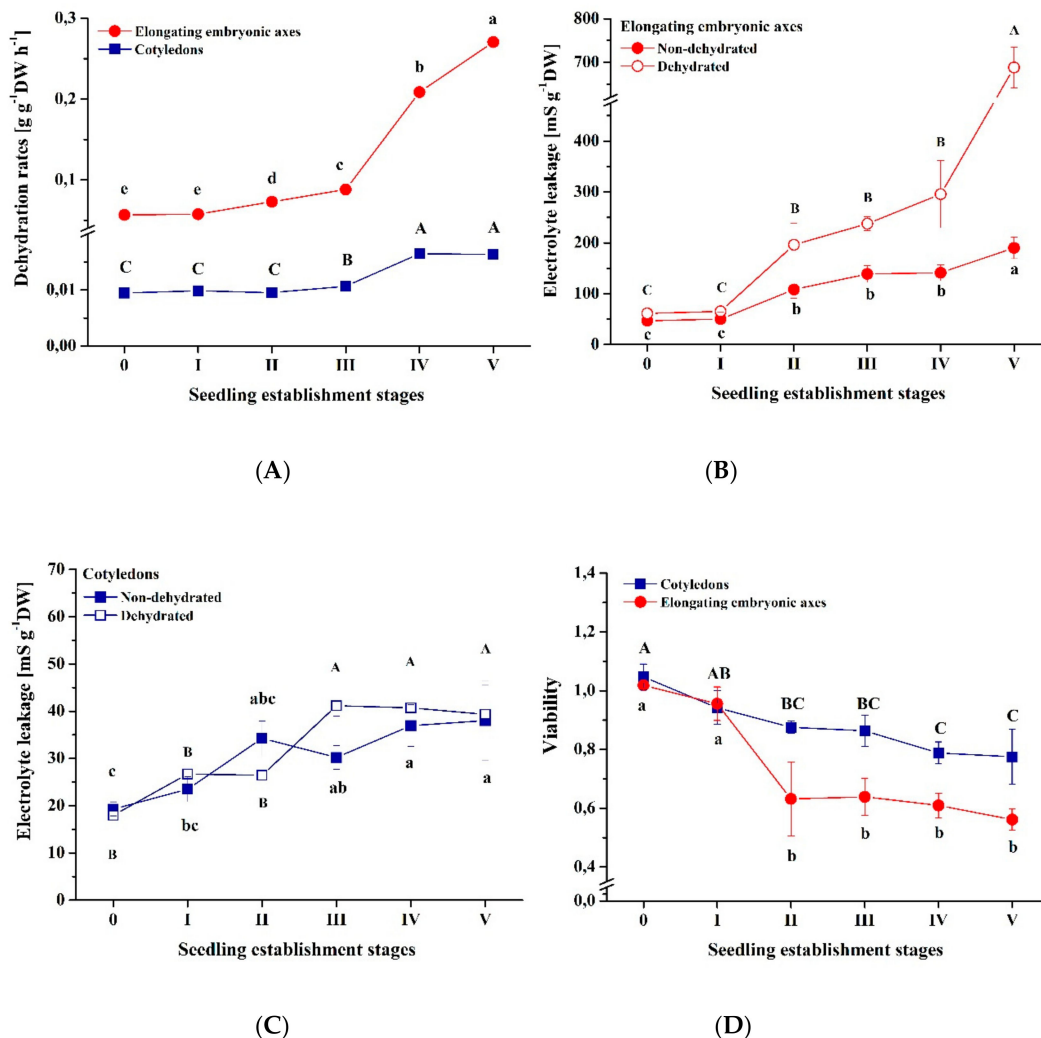


Figure 3. Changes in dehydration rates (A), electrolyte leakage before and after dehydration (B,C) and viability (D) of elongating embryonic axes and cotyledons of *Fagus sylvatica* reported at early seedling establishment stages. Data are the means of three independent replicates \pm the standard deviation. Statistically significant differences are indicated with different letters (one-way ANOVA followed by Tukey's test at $p \leq 0.05$).

Electrolyte leakage is one of the indexes of tissue viability. In dehydrated elongating embryonic axes, the increase of electrolyte leakage was more pronounced and increased nearly twofold at stages II-IV. Interestingly, membranes of dehydrated 25 mm elongating embryonic axes were highly permeable, and the electrolyte leakage was approximately four times higher compared to nondehydrated elongating embryonic axes at this stage and ten times higher compared to dehydrated elongating embryonic axes from 0-I stages. The electrolyte leakage gradually progressed in both nondehydrated and dehydrated cotyledons as the embryonic axes were prolonging and doubled at stage V compared to the initial values (Figure 3C). A significant increase in electrolyte leakage from dehydrated cotyledons was observed between stages II and III. In addition, the maximum value of electrolyte leakage detected in

cotyledons at stage IV and stage V was similar to the ones reported in elongating embryonic axes at stages 0-I.

Sensitivity to dehydration was tested separately in elongating embryonic axes and cotyledons because, during germination in the natural environment, the elongating embryonic axis is exposed to unfavorable conditions, whereas the cotyledon is protected by the testa. Sensitivity to dehydration was monitored before and after dehydration of seed tissues to 11% WC using the TTC dye test (Figure 3D, Figure S4), which is recommended for viability assessment in seed tissues. Before dehydration, both elongating embryonic axes and cotyledons were fully viable. After dehydration, the elongating embryonic axes were fully viable only during stages 0-I (Table S1). Elongating embryonic axes became visibly sensitive to dehydration upon reaching a length of 15 mm. In general, the apical parts containing radicles were not viable at seedling establishment stage III and beyond, indicating high sensitivity to dehydration. At seedling establishment stage III, the nonviable tissue extended beyond the root tip and included larger areas of radicles. The TTC test revealed that the tissue of the distal part of the elongating embryonic axis containing the radical is highly sensitive to dehydration. The viability was evaluated quantitatively and expressed as the viability ratio. The viability ratio equaled 1 in elongating embryonic axes at 0-I early seedling establishment stages (Figure 3D), reflecting 100% viability. At later stages, the viability decreased gradually and reached approximately 60% for dehydrated embryonic axes elongated to 20–25 mm. The surface of TTC-stained cotyledons was deep red at all analyzed early seedling establishment stages (Figure S4), whereas the cotyledon sections revealed a clear decrease in color intensity at stages III–IV, regardless of whether the dehydration treatment was applied. Nevertheless, dehydrated cotyledons began to lose their viability at stage II and attained approximately 80% viability at stage V (Figure 3D).

3.4. Chaperones

3.4.1. Dehydrin-like Proteins

Dehydrin-like proteins were barely detectable in the soluble fraction of proteins from both elongating embryonic axes (Figure 4A) and cotyledons (Figure 4D) of the germinating beech seeds. In elongating embryonic axes, a 44-kDa dehydrin protein was detectable only when heat-stable protein extract was used (Figure 4C). The level of the 44-kDa dehydrin decreased at seedling establishment stages I–III and was undetectable in 20 mm embryonic axes and longer (seedling establishment stages IV–V, data not shown). Dehydration induced the synthesis of a 44-kDa dehydrin and a 37-kDa dehydrin-like protein (Figure 4B,E). Pronounced reinduction of dehydrin protein synthesis was observed in the distal part of elongating embryonic axes containing the radicles compared to the apical part (Figure 4B). Interestingly, the 37-kDa protein level was the highest in elongating embryonic axes at seedling establishment stage I and then decreased. Dehydration caused notable induction of synthesis of 44- and 40-kDa proteins at seedling establishment stages 0-I, as well as a synthesis of 37-kDa dehydrin-like proteins at III-IV seedling establishment stages in cotyledons (Figure 4E).

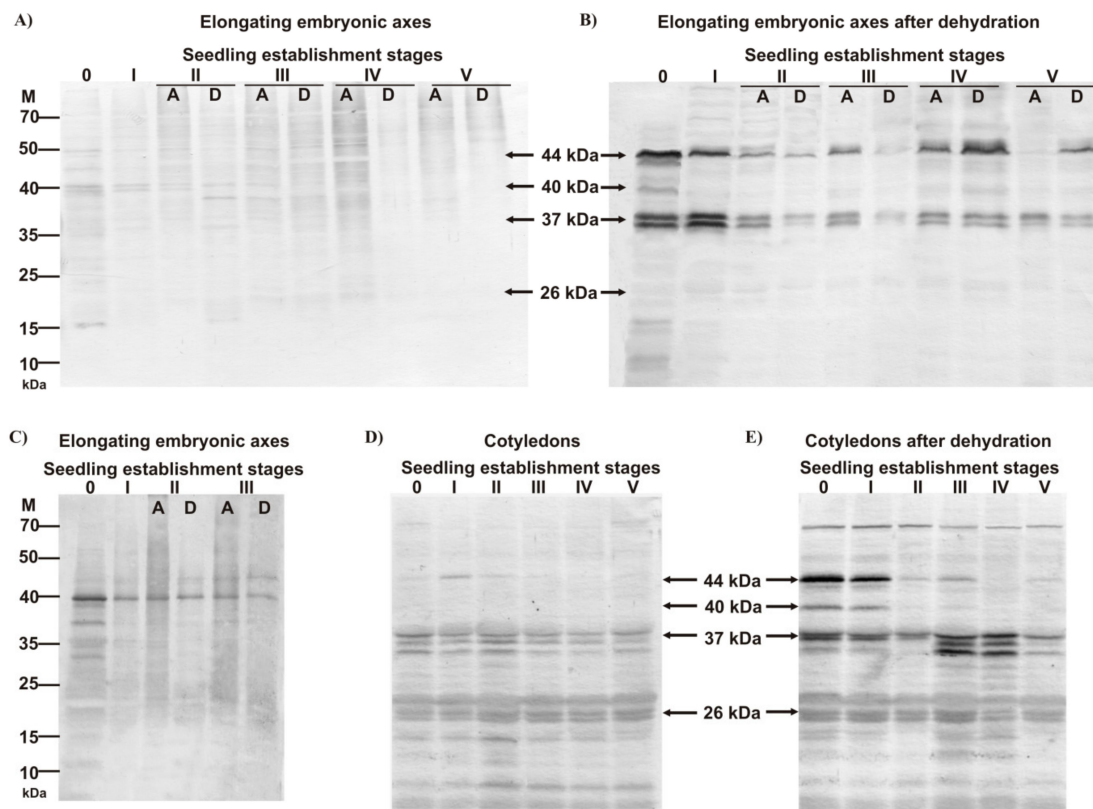


Figure 4. Detection of dehydrin-like proteins (indicated as arrows) in the elongating embryonic axes (A–C) and cotyledons (D–E) of germinated seeds and at early seedling establishment stages of *Fagus sylvatica* by Western blotting with antibodies specific to the K-segment before (A,D) and after dehydration to 11% of water content (B,E). Soluble (A,B,D,E) and heat-stable (C) protein extracts of 12.5 µg and 30 µg, respectively, were used. Each image is representative of three independent experiments with similar results. The Spectra™ multicolor broad range protein ladder standard was used to assess the molecular weight of the detected proteins. A, apical part of the elongating embryonic axes containing root tip of the radicle, D, distal part of the elongating embryonic axes containing hypocotyl.

3.4.2. Small Heat Shock Protein

The 22-kDa sHSP protein level decreased in elongating embryonic axes. The distal part referred to the radicles contained notably higher levels of this protein. However, the protein was not detectable in elongating embryonic axes that had protruded to 20–25 mm (Figure 5A). Dehydration caused a remarkable induction of 22-kDa sHSP synthesis, particularly at the 0–I seedling establishment stages (Figure 5B). At further stages, the level of the 22-kDa protein decreased but remained detectable at seedling establishment stages IV–V. In cotyledons, the 22-kDa protein was detected at notably low levels (Figure 5C). Dehydration intensified the synthesis of the 22-kDa protein at seedling establishment stages 0–I and reinduced at seedling establishment stage III (Figure 5D). At later seedling establishment stages, the protein gradually decreased.

At early beech seedling establishment stages, the production of H_2O_2 and $O_2^{\bullet-}$ was reported predominantly at the apical part of elongating embryonic axes referred to radicles (Figure 6). The area of both H_2O_2 and $O_2^{\bullet-}$ accumulation extended as the embryonic axes protruded and comprised nearly half the elongating embryonic axis length. The root tip was the location where $O_2^{\bullet-}$ was synthesized most abundantly at each stage. Dehydration changed the intensity and area of ROS production in an opposite manner. Dehydration resulted in a slight reduction of $O_2^{\bullet-}$ production in embryonic axes elongated to 3–7 mm and then the restriction of the region of $O_2^{\bullet-}$ production to the 1–2 mm area located at the root tip of radicle in embryonic axes elongated to 10–20 mm and complete blockage

of $O_2^{\bullet-}$ synthesis in embryonic axes elongated to 25 mm. In contrast, dehydration intensified the accumulation of H_2O_2 . At stage II and during further seedling establishment, the level of accumulated H_2O_2 increased dramatically. There were no such pronounced changes in cotyledons, except for the location where an elongating embryonic axis was connected to a cotyledon, where the latter did not show clear signs of ROS accumulation before and after dehydration (Figure S5).

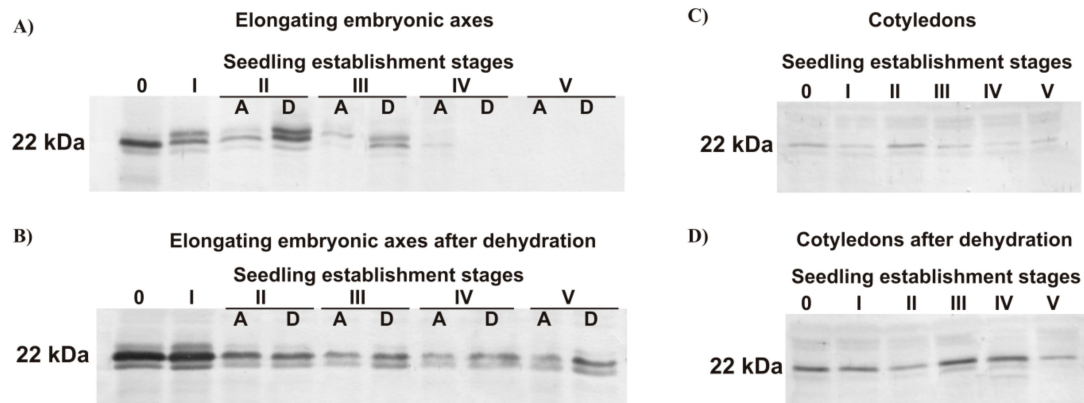


Figure 5. Detection of small heat shock protein (sHSP) in the elongating embryonic axes (A,B) and cotyledons (C,D) of germinated seeds and at early seedling establishment stages of *Fagus sylvatica* by Western blotting with antibodies specific to the *Arabidopsis* 17.4 sHSP before (A,C) and after dehydration to 11% of water content (B,D). Soluble protein extracts (12.5 μ g) were used. Each image is representative of three independent experiments with similar results. A, apical part of the elongating embryonic axes containing root tip of the radicle, D, distal part of the elongating embryonic axes containing hypocotyl. 3.5. ROS Production.

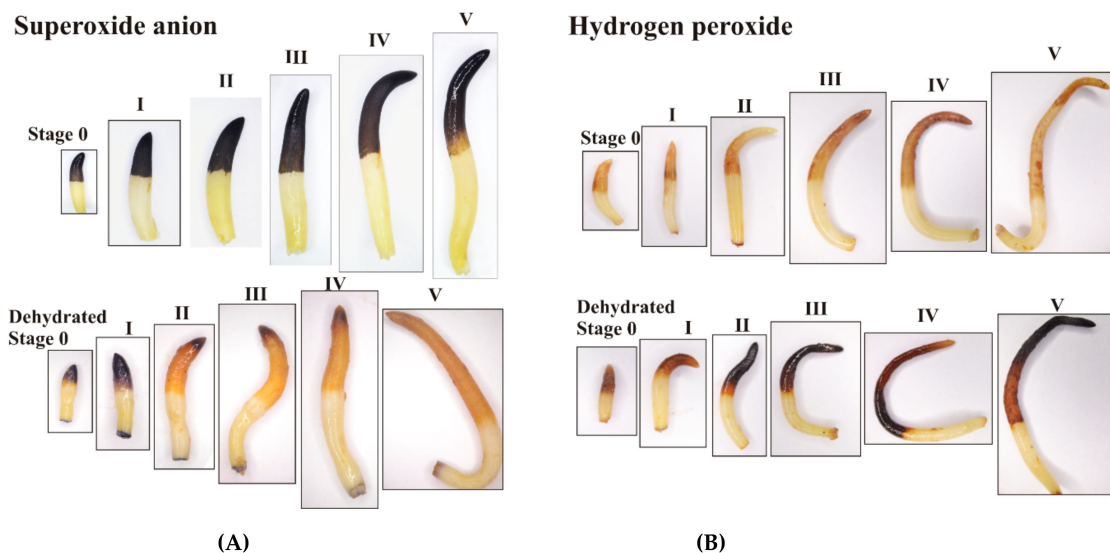


Figure 6. Histochemical detection of (A) superoxide anion radical ($O_2^{\bullet-}$) and (B) hydrogen peroxide (H_2O_2) in beech elongating embryonic axes at early seedling establishment 0-V stages before and after dehydration. H_2O_2 was visualized as reddish-brown stain, whereas $O_2^{\bullet-}$ was visualized as a black stain. A representative image of the elongating embryonic axis from each seedling establishment stage is given.

To summarize quantitatively determined parameters, the electrolyte leakage was strongly correlated ($R > 0.75$) with dehydration rates and viability in both cotyledons and radicles (Table S1). In radicles, the viability was also strongly correlated with the amounts of proteins and lipids. The amounts of both storage materials were strongly correlated with water content and electrolyte leakage.

4. Discussion

Drought and other climatic conditions reduce the establishment success of beech seedlings [49]. In particular, limited water affects the seed germination and seedling establishment process. Thus, dehydration sensitivity was examined at the early seedling establishment stages in this study. In cells of embryonic axes elongated to 20–25 mm, water constituted over 70% of FW. High water flux in elongating embryonic axes can be explained by the extreme permeability to water caused by cell wall integrity-related factors, such as extensins and expansins, which were reported to be differentially regulated during germination [27] and the highly water-permeable cubic lipid phase of the cell membrane characteristic of hydrated growing root cells [50], which was reflected in differences in electrolyte leakage and dehydration rates between elongating embryonic axes and less hydrated cotyledons. In cotyledons, numerous depositions of insoluble storage materials might contribute to the considerably delayed loss of tolerance to dehydration [1,12] compared to elongating embryonic axes [2,17]. Based on the lowest amounts of electrolyte leakage, which are related to desiccation tolerance in seeds [35,51], the level of tolerance to dehydration in cotyledons at 0-V stages was reported in elongating embryonic axes uniquely at 0-I stages.

After dehydration, fully viable elongating embryonic axes were reported at seedling establishment stages 0-I. A breakthrough was reported at stage II. Radicles then revealed evidence of deterioration, while the rates of dehydration and amounts of electrolyte leakage increased, making embryonic axes longer than 15 mm highly sensitive to environmental drought. At stages III–V, the apical part of the elongating embryonic axes referred to radicles became nonviable after dehydration, whereas the distal parts were fully viable in 15 mm-long embryonic axes and partially viable at further seedling establishment stages. In this context, the production of beech seedlings affected by drought conditions will depend on the possible formation of adventitious roots from the hypocotyl [52] because of the irreversible growth arrest of the primary root. Therefore, in beech seedlings, sensitivity to dehydration of radicles will largely define the dehydration tolerance limits.

Beech seeds accumulate lipids, mainly triacylglycerols [53,54] and proteins [54,55]. Cotyledons contained twice as many total proteins and lipids as elongating embryonic axes when germination third phase was initiated. Lipids constituted nearly 40% of the dry matter of cotyledons, which was also reflected in the ultrastructure of cotyledon cells. The size of oil bodies reported in beech seeds did not exceed 1.5 μm , which is in the referred range of 0.5 to 2.5 μm for oil bodies [56]. Ultrastructure analyses of beech cotyledon tissue showed that it was completely filled by oil bodies [54]. In this study, we showed that the contribution of oil bodies is different in particular cell layers. Oil bodies are predominantly more abundant in the external cell layers, forming a more solid matrix. In this regard, hydrophobic cortex stratum may protect cotyledon tissue from water loss as long as lipids are not consumed and affect dehydration tolerance, as indicated by Farrant et al. [12] and Walters [1]. This hypothesis is in keeping with the findings that accumulated insoluble reserves in seed tissues contribute to sensitivity to dehydration [12] and that genes categorized to the GO term lipid localization are involved in desiccation tolerance in seeds [17], as well as the fact that cotyledons of germinated orthodox seeds lose desiccation tolerance considerably later than embryonic axes [2,17].

Embryonic axes start to consume stored lipids as energy and carbon skeleton sources earlier than cotyledons [57] and that the energy and carbon were used for beech embryonic axis protrusion ($r = -0.7006$, $p = 0.003625$) and were related to viability. Changes in lipid content in embryonic axes and, to a greater extent, in elongating embryonic axes might be related to the regulation of dormancy release and germination processes because lipids were reported to be involved in signaling processes [58]. Metabolite mapping and profiling during seed germination showed that changes in the localization and distribution of oils, including triacylglycerols, fatty acids, and phospholipids, are important for the germination process [57]. In this regard, lipid-associated signaling events linked to dormancy release probably began during the stratification process primarily in embryonic axes, enabling germination and elongation of embryonic axes.

Transcriptomic [2,16,17] and proteomic [59] analyses led to the identification of genes and proteins particularly important for desiccation tolerance in seeds and germination. The decline and disappearance of some LEA proteins are linked to desiccation tolerance loss in seeds [15,16,19,59], and dehydrins are differentially expressed in desiccation tolerant and desiccation sensitive seed tissues [2,17]. Compared to developing [23] and dry beech seeds [22], germinating seeds and seedlings contained very low levels of the 44-kDa dehydrin, indicating that the desiccation tolerance was probably lost at earlier stages than studied in this report. It was reported that 44-kDa dehydrin protein synthesis is induced by drying and/or ABA [3], and its transcript level is highly correlated with dehydration levels [23]. The 37-kDa dehydrin-like protein was not previously detected at such a high level in beech seeds and became an interesting candidate for more detailed research. The constant level of the 37-kDa protein in maturing embryonic axes [21] suggests that the expression of this protein was not related to decreasing water content. Two bands of the 37-kDa dehydrin candidates in elongating embryonic axes and three in cotyledons might be attributable to tissue-specific forms of alternative splicing, as was reported in YK dehydrin in drought-treated plant tissues [24], as well as different posttranslational modifications of 37-kDa dehydrin candidate, including phosphorylation, that are possible in dehydrins [23]. The synthesis of the 37-kDa dehydrin candidates was induced uniquely at seedling establishment stages III-IV in cotyledons. In these seedling establishment stages, water loss was the most intense, and cotyledons strongly responded to dehydration. Beyond the intense synthesis of the 37-kDa dehydrin-like protein, dehydration also caused a remarkable increase of the 22-kDa sHSP protein. Moreover, at the edge of seedling establishment stage III/IV, the total protein level decreased significantly, suggesting intensified protein metabolism at this specific time point of seedling establishment.

HSPs contribute to general stress alleviation not only in seeds [18]. However, the expression of some HSP genes is linked to dehydration [2,17] and decreases after germination [26]. Enhanced tolerance to severe dehydration was reported in sunflower seedlings after overexpression of two heat shock factors [60]. Accumulation of the 22-kDa sHSP in maturing beech embryonic axes (Figure S6) is in keeping with the finding that the synthesis of sHSPs is part of the seed developmental program when desiccation tolerance is acquired [25]. Dehydration intensified the synthesis of the 22-kDa sHSP at all tested seedling establishment stages. This chaperone protection may be helpful for beech seedling formation uniquely at temporary shortages of water because 22-kDa sHSP decreased in radicles either under physiological and desiccation conditions. Based on the results of Kaur et al. [26], in which the expression of OsHSP18.2 in *A. thaliana* seeds resulted in improved vigor, longevity and seedling establishment under abiotic stress conditions, the specific function of sHSPs in seeds at different physiological stages remains to be fully explored.

Isolation of the embryonic axis the seed is perceived as wounding, and ROS production usually occurs at the cut surface [61]. This phenomenon will not be discussed in this report. Abundantly accumulated $O_2^{\bullet-}$ in nondehydrated elongating embryonic axes is suggested to have a signaling role during seedling establishment. This hypothesis is consistent with Singh et al. [62], who demonstrated that postgerminative axis growth requires $O_2^{\bullet-}$, which accumulates in the root tip of the radicle emerging from the seed, and with Kranner et al. [63], who established that radicle elongation is accompanied by an increase in $O_2^{\bullet-}$ production. ROS homeostasis is important in modulating the root growth process. H_2O_2 produced in the elongation zone is involved in cell differentiation, whereas $O_2^{\bullet-}$ synthesized in the transition zone acts in cell proliferation [33]. In this context, decreased $O_2^{\bullet-}$ levels and further the absence of $O_2^{\bullet-}$ in dehydrated 25 mm beech embryonic axes possibly lead to cellular redox alternations and inhibition of root growth and development because $O_2^{\bullet-}$, produced by NADPH oxidases, was reported as necessary for root development and elongation [31]. ROS signaling is restricted to hydrated zones [64]. Thus, dehydrated 10 mm and longer beech embryonic axes are not able to continue growth processes because the levels of $O_2^{\bullet-}$ detected in the quiescent center (QC) area of embryonic axes elongated to 10–20 mm are probably too low for cell division processes in QC and cell proliferation at the transition zone. Stress factors can gradually reduce $O_2^{\bullet-}$ production

required for normal root growth in the apex region, thereby disturbing ROS homeostasis and root morphogenesis [65]. A dehydration-induced similar phenomenon was observed in beech elongating embryonic axes.

The accumulation of ROS above a specific threshold level switches the ROS function from a useful signaling molecule to a deleterious one [14,30,63]. H₂O₂ overproduction detected in radicles of elongating embryonic axes at the II-V early seedling establishment stages is probably linked to oxidative stress that occurs in dehydration-sensitive seed tissues [35] because enhanced H₂O₂ production is not the element of the radicle elongation program [63]. In keeping with our results, increased amounts of electrolyte leakage were reported to be correlated with lowered viability in dehydrated seeds sensitive to desiccation [37,39,40] and contributed to formulating the cause-and-effect sequence, confirming experimentally that declined viability is driven by H₂O₂ accumulation followed by elevated electrolyte leakage [37,40]. H₂O₂ diffuses across cell membranes through the aquaporin channels [66] and spreads freely through disintegrated membranes in damaged tissue. Based on our previous studies of beech seed aging, the QC, an initial area of the apical meristem, was found to be a region accumulating ROS during seed storage and aging [14]. Moreover, higher ROS levels were associated with lower seed germinability [14]. Thus, we hypothesize that dehydration-initiated excessively low O₂^{•-} levels and excessively high H₂O₂ levels are out of a favorable range of ROS concentrations required for seedling growth and development, thereby affecting the viability and beech seedling performance. Simultaneous overproduction of H₂O₂ and O₂^{•-} depletion in dehydrated elongating embryonic axes is possible because auxin stimulating plant peroxidases can generate O₂^{•-} in an H₂O₂-independent manner [67]. Auxins, via redox intermediates, are involved in the organization of the QC oxidizing environment therein [68]. In this context, O₂^{•-} production in protruding embryonic axes might originate from the abovementioned pathway.

Recent studies revealed that dehydrins protect DNA from ROS [69]. Such protection may be sustained in beech elongating embryonic axes at 0-I stages because dehydrins were reported to localize in the nucleus of beech embryonic axes [21]. The expression of peroxidases responsible for the modulation of ROS levels controlling the transition from proliferation to differentiation in the root is regulated in germinating seeds by specific transcription factors [33]. From this perspective, gene expression as the element of the program of seedling performance might be promoted by dehydrins and further disturbed by water stress and subsequent oxidative stress. Dehydrins are involved in protection against oxidative stress by reducing H₂O₂ levels and enhancing the expression of ROS scavenging enzymes [70]. Conversely, suppressed expression of ROS scavenging enzymes, including superoxide dismutase and peroxidase, leading to ROS accumulation was reported in dehydrin-silenced pepper plants [71]. In this context, the link between dehydrins and ROS warrants further research.

5. Conclusions

Desiccation tolerance enables the survival of organisms and tissues exposed to severe dehydration. Desiccation-tolerant seeds become sensitive to desiccation upon germination, thus, seedlings at early establishment stages are exceptionally sensitive to environmental drought, particularly the primary root, because cotyledons are more tolerant to dehydration than radicles. Important physiological stages and transitions in seeds, as well as stress conditions, introduce changes associated with distinct gene expression and metabolic switches. All molecules and cellular structures involved in the events require extended protection provided by e.g. protein chaperones, such as LEAs and HSPs. Storage material consumption and growth were initiated in embryonic axes, thus, sensitivity to dehydration occurred earlier in elongating embryonic axes than in cotyledons. Dehydration rates in elongating embryonic axes and cotyledons were driven by distinct hydration and storage material content and the arrangement of oil bodies. In cotyledons, the external layer of cells filled almost completely with storage materials, mainly oil bodies, might function as a barrier to water loss. In elongating embryonic axes, tolerance to dehydration was supported until the dehydrin-like proteins and sHSP decreased and disappeared. Environmental drought may limit seedling growth and performance

because dehydration-induced chaperone synthesis is transient, insufficient and completely inverse to ROS production in radicles. ROS perturbations manifested by H₂O₂ overproduction and O₂^{•−} deficiency have been reported since the II stage and intensified at further seedling establishment stages. The function of the germination control center cannot be sustained in the nonviable root tips because the apical part of elongating embryonic axes containing radicles is the most sensitive part of the seed to dehydration. The resistance to dehydration might be sustained until embryonic axes reach 10 mm - the unique stages in which the environmental drought has no impact on beech seedling performance. The further seedling formation is completely dependent on environmental drought, which implies ROS imbalance and reduced viability. We showed statistical evidence that the viability of elongating embryonic axes is driven by water content, dehydration rates, electrolyte leakage, and protein and lipid amounts, as well as H₂O₂-induced oxidative damage, which can be deduced from ROS histochemical localization. To increase the success of beech seedling performance, watering should be considered combined with site preparation in the natural regeneration of beech trees, and balanced water regimes should be kept in forest-tree nurseries to prevent dehydration stress and the consequences described in our study.

Supplementary Materials: The following are available online at <http://www.mdpi.com/1999-4907/10/10/900/s1>, Figure S1: Experiment scheme, Figure S2: Detection of lipids, Figure S3: Dynamics of dehydration, Figure S4: Determination of dehydration tolerance using the TTC test, Figure S5: Histochemical detection of ROS, Figure S6: Detection of small heat shock protein, Table S1: Correlation coefficient.

Author Contributions: Conceptualization, A.B.-Z., E.M.K., and S.P.; funding acquisition and project administration, E.M.K. and S.P.; experimental implementation, E.M.K., A.B.-Z., and J.S.; data analyses, E.M.K., A.B.-Z.; writing—original draft preparation, E.M.K.; writing—review and editing, A.B.-Z., E.M.K., J.S. and S.P.

Funding: This research was supported by the Ministry of Science and Information (Poland) grant No. 2PO6L02927 and the Ministry of Science and Higher Education (Poland) / National Science Centre (Poland) grant No. N N309 136535. Additional funding was provided by the Institute of Dendrology of the Polish Academy of Sciences.

Acknowledgments: The antisera raised against the K segment were generously supplied by T.J. Close from the Department of Botany and Plant Sciences at the University of California, Riverside, CA, USA. The antisera raised against the Arabidopsis anti-Hsp17.4 were generously supplied by E. Vierling from the Department of Biochemistry and Molecular Biophysics at the University of Arizona, Tucson, AZ, USA.

Conflicts of Interest: The authors declare no conflict of interest.

References

1. Walters, C. Orthodoxy, recalcitrance and in-between: Describing variation in seed storage characteristics using threshold responses to water loss. *Planta* **2015**, *242*, 397–406. [[CrossRef](#)] [[PubMed](#)]
2. Buitink, J.; Vu, B.L.; Satour, P.; Leprince, O. The re-establishment of desiccation tolerance in germinated radicles of *Medicago truncatula* Gaertn. seeds. *Seed Sci. Res.* **2003**, *13*, 273–286. [[CrossRef](#)]
3. Kalembe, E.M.; Janowiak, F.; Pukacka, S. Desiccation tolerance acquisition in developing beech (*Fagus sylvatica* L.) seeds: The contribution of dehydrin-like protein. *Trees* **2009**, *23*, 305–315. [[CrossRef](#)]
4. León-Lobos, P.; Ellis, R.H. Seed storage behaviour of *Fagus sylvatica* and *Fagus crenata*. *Seed Sci. Res.* **2002**, *12*, 31–37. [[CrossRef](#)]
5. Bogdziewicz, M.; Szymkowiak, J.; Kasprzyk, I.; Grewling, L.; Borowski, Z.; Borycka, K.; Kantorowicz, W.; Myszowska, D.; Piotrowicz, K.; Ziemianin, M.; et al. Masting in wind-pollinated trees: The role of weather and pollination dynamics in driving seed production. *Ecology* **2017**, *98*, 2615–2625. [[CrossRef](#)] [[PubMed](#)]
6. Augustaitis, A.; Jasineviciene, D.; Girgzdiene, R.; Kliucius, A.; Marozas, V. Sensitivity of beech trees to global environmental changes at most north-eastern latitude of their occurrence in Europe. *Sci. World J.* **2012**, *2012*, 743926. [[CrossRef](#)] [[PubMed](#)]
7. Pukacka, S.; Hoffmann, S.K.; Goslar, J.; Pukacki, P.M.; Wójkiewicz, E. Water and lipid relations in beech (*Fagus sylvatica* L.) seeds and its effect on storage behaviour. *Biochim. Biophys. Acta* **2003**, *1621*, 48–56. [[CrossRef](#)]
8. Övergaard, R.; Agestam, E.; Ekö, P.M. Seed production and natural regeneration of beech (*Fagus sylvatica* L.) in southern Sweden. *Stud. For. Suec.* **2009**, *218*, 1–30.

9. Tang, J.; Busso, C.A.; Jiang, D.; Wang, Y.; Wu, D.; Musa, A.; Miao, R.; Miao, C. Seed burial depth and soil water content affect seedling emergence and growth of *Ulmus pumila* var. *sabulosa* in the Horqin Sandy Land. *Sustainability* **2016**, *8*, 68.
10. Bewley, J.D.; Bradford, K.J.; Hilhorst, H.W.M.; Nonogaki, H. *Seeds: Physiology of Development; Germination and Dormancy*, 3rd ed.; Springer: New York, NY, USA, 2013.
11. Penfield, S.; Graham, S.; Graham, I.A. Storage reserve mobilization in germinating oilseeds: Arabidopsis as a model system. *Biochem. Soc. Trans.* **2005**, *33*, 380–383. [[CrossRef](#)]
12. Farrant, J.; Pammenter, N.; Berjak, P.; Walters, C. Subcellular organization and metabolic activity during the development of seeds that attain different levels of desiccation tolerance. *Seed Sci. Res.* **1997**, *7*, 135–144. [[CrossRef](#)]
13. Ratajczak, E.; Pukacka, S. Decrease in beech (*Fagus sylvatica*) seed viability caused by temperature and humidity conditions as related to membrane damage and lipid composition. *Acta Physiol. Plant.* **2005**, *27*, 3–11. [[CrossRef](#)]
14. Ratajczak, E.; Kalembe, E.M.; Pukacka, S. Age-related changes in protein metabolism of beech (*Fagus sylvatica* L.) seeds during alleviation of dormancy and in the early stage of germination. *Plant. Physiol. Biochem.* **2015**, *94*, 114–121. [[CrossRef](#)] [[PubMed](#)]
15. Dekkers, B.J.; Costa, M.C.; Maia, J.; Bentsink, L.; Ligterink, W.; Hilhorst, H.W. Acquisition and loss of desiccation tolerance in seeds: From experimental model to biological relevance. *Planta* **2015**, *241*, 563–577. [[CrossRef](#)] [[PubMed](#)]
16. Costa, M.C.D.; Righetti, K.; Nijveen, H.; Yazdanpanah, F.; Ligterink, W.; Buitink, J.; Hilhorst, H.W.M. A gene co-expression network predicts functional genes controlling the re-establishment of desiccation tolerance in germinated *Arabidopsis thaliana* seeds. *Planta* **2015**, *242*, 435–449. [[CrossRef](#)] [[PubMed](#)]
17. Maia, J.; Dekkers, B.J.; Provart, N.J.; Ligterink, W.; Hilhorst, H.W. The re-establishment of desiccation tolerance in germinated *Arabidopsis thaliana* seeds and its associated transcriptome. *PLoS ONE* **2011**, *6*, e29123. [[CrossRef](#)] [[PubMed](#)]
18. Wang, W.; Vinocur, B.; Shoseyov, O.; Altman, A. Role of plant heat-shock proteins and molecular chaperones in the abiotic stress response. *Trends Plant. Sci.* **2004**, *9*, 244–252. [[CrossRef](#)]
19. Radwan, A.; Hara, M.; Kleinwächter, M.; Selmar, D. Dehydrin expression in seeds and maturation drying: A paradigm change. *Plant. Biol. (Stuttg)* **2014**, *16*, 853–855. [[CrossRef](#)]
20. Close, T.J.; Fenton, R.D.; Moonan, F. A view of plant dehydrins using antibodies specific to the carboxy terminal peptide. *Plant. Mol. Biol.* **1993**, *23*, 279–286. [[CrossRef](#)]
21. Kalembe, E.M.; Bagniewska-Zadworna, A.; Ratajczak, E. Multiple subcellular localizations of dehydrin-like proteins in the embryonic axes of common beech (*Fagus sylvatica* L.) seeds during maturation and dry storage. *J. Plant. Growth Regul.* **2015**, *34*, 137–149. [[CrossRef](#)]
22. Kalembe, E.M.; Pukacka, S. Changes in late embryogenesis abundant proteins and a small heat shock protein during storage of beech (*Fagus sylvatica* L.) seeds. *Environ. Exp. Bot.* **2008**, *63*, 274–280. [[CrossRef](#)]
23. Kalembe, E.M.; Litkowiec, M. Functional characterization of a dehydrin protein from *Fagus sylvatica* seeds using experimental and in silico approaches. *Plant. Physiol. Biochem.* **2015**, *97*, 246–254. [[CrossRef](#)] [[PubMed](#)]
24. Vaseva, I.I.; Anders, I.; Feller, U. Identification and expression of different dehydrin subclasses involved in the drought response of *Trifolium repens*. *J. Plant. Physiol.* **2014**, *171*, 213–224. [[CrossRef](#)] [[PubMed](#)]
25. Wehmeyer, N.; Hernandez, L.D.; Finkelstein, R.R.; Vierling, E. Synthesis of small heat-shock proteins is part of the developmental program of late seed maturation. *Plant. Physiol.* **1996**, *112*, 747–757. [[CrossRef](#)] [[PubMed](#)]
26. Kaur, H.; Petla, B.P.; Kamble, N.U.; Singh, A.; Rao, V.; Salvi, P.; Ghosh, S.; Majee, M. Differentially expressed seed aging responsive heat shock protein OsHSP18.2 implicates in seed vigor; longevity and improves germination and seedling establishment under abiotic stress. *Front. Plant. Sci.* **2015**, *6*, 713. [[CrossRef](#)] [[PubMed](#)]
27. Tan, L.; Chen, S.; Wang, T.; Dai, S. Proteomic insights into seed germination in response to environmental factors. *Proteomics* **2013**, *13*, 1850–1870. [[CrossRef](#)] [[PubMed](#)]
28. Kalembe, E.M.; Pukacka, S. Carbonylated proteins accumulated as vitality decreases during long-term storage of beech (*Fagus sylvatica* L.) seeds. *Trees* **2014**, *28*, 503–515. [[CrossRef](#)]
29. Jeevan Kumar, S.P.; Rajendra Prasad, S.; Banerjee, R.; Thammineni, C. Seed birth to death: Dual functions of reactive oxygen species in seed physiology. *Ann. Bot.* **2015**, *116*, 663–668. [[CrossRef](#)]

30. Bailly, C.; El-Maarouf-Bouteau, H.; Corbineau, F. From intracellular signaling networks to cell death, the dual role of reactive oxygen species in seed physiology. *C. R. Biol.* **2008**, *331*, 806–814. [[CrossRef](#)]
31. Kwak, J.M.; Mori, I.C.; Pei, Z.M.; Leonhardt, N.; Torres, M.A.; Dang, J.L.; Bloom, R.E.; Bodde, S.; Jones, J.D.G.; Schroeder, J.I. NADPH oxidase *AtrbohD* and *AtrbohF* genes function in ROS-dependent ABA signaling in *Arabidopsis*. *EMBO J.* **2003**, *22*, 2623–2633. [[CrossRef](#)]
32. Liskay, A.; van der Zalm, E.; Schopfer, P. Production of reactive oxygen intermediates (O_2^- ; H_2O_2 ; and $\cdot OH$) by maize roots and their role in wall loosening and elongation growth. *Plant. Physiol.* **2004**, *136*, 3114–3123. [[CrossRef](#)] [[PubMed](#)]
33. Tsukagoshi, H.; Busch, W.; Benfey, P.N. Transcriptional regulation of ROS controls transition from proliferation to differentiation in the root. *Cell* **2010**, *143*, 606–616. [[CrossRef](#)] [[PubMed](#)]
34. Schopfer, P.; Plachy, C.; Frahry, G. Release of reactive oxygen intermediates (superoxide radicals, hydrogen peroxide, and hydroxyl radicals) and peroxidase in germinating radish seeds controlled by light, gibberellin, and abscisic acid. *Plant. Physiol.* **2001**, *125*, 1591–1602. [[CrossRef](#)] [[PubMed](#)]
35. Pukacka, S.; Ratajczak, E. Ascorbate and glutathione metabolism during development and desiccation of orthodox and recalcitrant seeds of the genus *Acer*. *Funct. Plant. Biol.* **2007**, *34*, 601–613. [[CrossRef](#)]
36. Pukacka, S.; Ratajczak, E. Age-related biochemical changes during storage of beech (*Fagus sylvatica* L.) seeds. *Seed Sci. Res.* **2007**, *17*, 45–53. [[CrossRef](#)]
37. Chandra, J.; Keshavkant, S. Desiccation-induced ROS accumulation and lipid catabolism in recalcitrant *Madhuca latifolia* seeds. *Physiol. Mol. Biol. Plants* **2018**, *24*, 75–87. [[CrossRef](#)] [[PubMed](#)]
38. Sershen; Varghese, B.; Naidoo, C.; Pammenter, N.W. The use of plant stress biomarkers in assessing the effects of desiccation in zygotic embryos from recalcitrant seeds: Challenges and considerations. *Plant. Biol. (Stuttg)* **2016**, *18*, 433–444. [[CrossRef](#)]
39. Li, C.; Sun, W.Q. Desiccation sensitivity and activities of free radical scavenging enzymes in recalcitrant *Theobroma cacao* seeds. *Seed Sci. Res.* **1999**, *9*, 209–217. [[CrossRef](#)]
40. Kalembe, E.M.; Ratajczak, E. The effect of a doubled glutathione level on parameters affecting the germinability of recalcitrant *Acer saccharinum* seeds during drying. *J. Plant. Physiol.* **2018**, *223*, 72–83. [[CrossRef](#)]
41. Topham, A.T.; Taylor, R.E.; Yan, D.; Nambara, E.; Johnston, I.G.; Bassel, G.W. Temperature variability is integrated by a spatially embedded decision-making center to break dormancy in *Arabidopsis* seeds. *Proc. Natl. Acad. Sci. USA* **2017**, *114*, 6629–6634. [[CrossRef](#)]
42. Sliwinska, E.; Bassel, G.W.; Bewley, J.D. Germination of *Arabidopsis thaliana* seeds is not completed as a result of elongation of the radicle but of the adjacent transition zone and lower hypocotyl. *J. Exp. Bot.* **2009**, *60*, 3587–3594. [[CrossRef](#)] [[PubMed](#)]
43. *International Rules for Seed Testing; The Topographical Tetrazolium Test*; The International Seed Testing Association (ISTA): Bassersdorf, Switzerland, 2016; p. i-6-26.
44. Chen, W.P.; Li, P.H.; Chen, T.H.H. Glycinebetaine increases chilling tolerance and reduces chilling-induced lipid peroxidation in *Zea mays* L. *Plant. Cell Environ.* **2000**, *23*, 609–618. [[CrossRef](#)]
45. Bagniewska-Zadworna, A.; Wojciechowicz, M.K.; Zenkteler, M.; Jeżowski, S.; Zenkteler, E. Cytological analysis of hybrid embryos of Intergeneric crosses between *Salix viminalis* and *Populus* species. *Austr. J. Bot.* **2010**, *58*, 42–48. [[CrossRef](#)]
46. Krishnamurthy, K.V. *Methods in Cell Wall Cytochemistry*; CRC Press: Boca Raton, FL, USA, 1999.
47. Daudi, A.; O'Brien, J.A. Detection of hydrogen peroxide by DAB staining in *Arabidopsis* Leaves. *Bio. Protoc.* **2012**, *2*, e263. [[CrossRef](#)] [[PubMed](#)]
48. Kumar, D.; Yusuf, M.A.; Singh, P.; Sardar, M.; Sarin, N.B. Histochemical detection of superoxide and H_2O_2 accumulation in *Brassica juncea* seedlings. *Bio. Protoc.* **2014**, *4*, e1108. [[CrossRef](#)]
49. Robson, T.M.; Rodríguez-Calcerrada, J.; Sánchez-Gómez, D.; Aranda, I. Summer drought impedes beech seedling performance more in a sub-Mediterranean forest understory than in small gaps. *Tree Physiol.* **2009**, *29*, 249–259. [[CrossRef](#)]
50. Norberg, P.; Liljeborg, C. Lipids of plasma membranes prepared from oat root cells: effects of induced water-deficit tolerance. *Plant. Physiol.* **1991**, *96*, 1136–1141. [[CrossRef](#)]
51. Sun, W.Q.; Leopold, A.C. Acquisition of desiccation tolerance in soybeans. *Physiol. Plant.* **1993**, *87*, 403–409. [[CrossRef](#)]

52. Da Costa, C.T.; de Almeida, M.R.; Ruedell, C.M.; Schwambach, J.; Maraschin, F.S.; Fett-Neto, A.G. When stress and development go hand in hand: Main hormonal controls of adventitious rooting in cuttings. *Front. Plant. Sci.* **2013**, *4*, 133. [[CrossRef](#)]
53. Prasad, R.B.N.; Guelz, P.G. Composition of lipids of beech *Fagus sylvatica* L. seed oil. *Zeitschrift fuer Naturforschung C* **1989**, *44*, 735–738. [[CrossRef](#)]
54. Collada, C.; Aragoncillo, P.; Aragoncillo, C. Development of protein bodies in cotyledons of *Fagus sylvatica*. *Physiol. Plant.* **1993**, *89*, 354–359. [[CrossRef](#)]
55. Eliasova, K.; Pesek, B.; Vondrakova, Z. Storage compounds, ABA and fumarase in *Fagus sylvatica* embryos during stratification. *Dendrobiology* **2015**, *74*, 25–33. [[CrossRef](#)]
56. Murphy, D.J. *Plant Lipids, Biology, Utilisation and Manipulation*; Blackwells: Oxford, UK, 2004.
57. Feenstra, A.D.; Alexander, L.E.; Song, Z.; Korte, A.R.; Yandea-Nelson, M.D.; Nikolau, B.J.; Lee, Y.J. Spatial mapping and profiling of metabolite distributions during germination. *Plant. Physiol.* **2017**, *174*, 2532–2548. [[CrossRef](#)] [[PubMed](#)]
58. Van der Schoot, C.; Paul, L.K.; Paul, S.B.; Rinne, P.L. Plant lipid bodies and cell-cell signaling: A new role for an old organelle? *Plant. Signal. Behav.* **2011**, *6*, 1732–1738. [[CrossRef](#)] [[PubMed](#)]
59. Wang, W.Q.; Liu, S.J.; Song, S.Q.; Møller, I.M. Proteomics of seed development, desiccation tolerance, germination and vigor. *Plant. Physiol. Biochem.* **2015**, *86*, 1–15. [[CrossRef](#)] [[PubMed](#)]
60. Personat, J.M.; Tejedor-Cano, J.; Prieto-Dapena, P.; Almoguera, C.; Jordano, J. Co-overexpression of two Heat Shock Factors results in enhanced seed longevity and in synergistic effects on seedling tolerance to severe dehydration and oxidative stress. *BMC Plant. Biol.* **2014**, *14*, 56. [[CrossRef](#)] [[PubMed](#)]
61. Roach, T.; Ivanova, M.; Beckett, R.P.; Minibayeva, F.V.; Green, I.; Pritchard, H.W.; Kranner, I. An oxidative burst of superoxide in embryonic axes of recalcitrant sweet chestnut seeds as induced by excision and desiccation. *Physiol. Plant.* **2008**, *133*, 131–139. [[CrossRef](#)]
62. Singh, K.L.; Chaudhuri, A.; Kar, R.K. Superoxide and its metabolism during germination and axis growth of *Vigna radiata* (L.) Wilczek seeds. *Plant. Signal. Behav.* **2014**, *9*, e29278. [[CrossRef](#)]
63. Kranner, I.; Roach, T.; Beckett, R.P.; Whitaker, C.; Minibayeva, F.V. Extracellular production of reactive oxygen species during seed germination and early seedling growth in *Pisum sativum*. *J. Plant. Physiol.* **2010**, *167*, 805–811. [[CrossRef](#)]
64. El-Maarouf-Bouteau, H.; Bailly, C. Oxidative signaling in seed germination and dormancy. *Plant. Signal. Behav.* **2008**, *3*, 175–182. [[CrossRef](#)]
65. Kagenishi, T.; Yokawa, K.; Baluška, F. MES buffer affects Arabidopsis root apex zonation and root growth by suppressing superoxide generation in root apex. *Front. Plant. Sci.* **2016**, *7*, 79. [[CrossRef](#)] [[PubMed](#)]
66. Tamma, G.; Valenti, G.; Grossini, E.; Donnini, S.; Marino, A.; Marinelli, R.A.; Calamita, G. Aquaporin membrane channels in oxidative stress, cell signaling, and aging: recent advances and research trends. *Oxidative Med. Cell Longev.* **2018**, 1501847. [[CrossRef](#)] [[PubMed](#)]
67. Kimura, M.; Umemoto, Y.; Kawano, T. Hydrogen peroxide-independent generation of superoxide by plant peroxidase: Hypotheses and supportive data employing ferrous ion as a model stimulus. *Front. Plant. Sci.* **2014**, *5*, 285. [[CrossRef](#)] [[PubMed](#)]
68. Jiang, K.; Meng, Y.L.; Feldman, L.J. Quiescent center formation in maize roots is associated with an auxin-regulated oxidizing environment. *Development* **2003**, *130*, 1429–1438. [[CrossRef](#)] [[PubMed](#)]
69. Boddington, K.F.; Graether, S.P. Binding of a *Vitis riparia* dehydrin to DNA. *Plant. Sci.* **2019**, *287*, 110172. [[CrossRef](#)] [[PubMed](#)]
70. Halder, T.; Upadhyaya, G.; Basak, C.; Das, A.; Chakraborty, C.; Ray, S. Dehydrins impart protection against oxidative stress in transgenic tobacco plants. *Front. Plant. Sci.* **2018**, *9*, 136. [[CrossRef](#)] [[PubMed](#)]
71. Luo, D.; Hou, X.; Zhang, Y.; Meng, Y.; Zhang, H.; Liu, S.; Wang, X.; Chen, R. CaDHN5, a dehydrin gene from pepper, plays an important role in salt and osmotic stress responses. *Int. J. Mol. Sci.* **2019**, *20*, 1989. [[CrossRef](#)]

